Egyptian Journal of Basic and Applied Sciences 4 (2017) 249–255

HOSTED BY

Contents lists available at ScienceDirect

Egyptian Journal of Basic and Applied Sciences

journal homepage: www.elsevier.com/locate/ejbas

Full Length Article

Efficacy of silver nanoparticles mediated by *Jania rubens* and *Sargassum dentifolium* macroalgae; Characterization and biomedical applications

Hani Saber [a], Eman A. Alwaleed [a], K.A. Ebnalwaled [b,c], Asmaa Sayed [a], Wesam Salem [a,*]

[a] Botany Department, Faculty of Science, South Valley University, Qena 83523, Egypt
[b] Electronics & Nano Devices Laboratory, Physics Department, Faculty of Science, South Valley University, Qena 83523, Egypt
[c] Egypt Nanotechnology Center (EGNC), Cairo University Sheikh Zayed Campus, 12588 Giza, Egypt

ARTICLE INFO

Article history:
Received 5 August 2017
Received in revised form 7 October 2017
Accepted 17 October 2017
Available online 31 October 2017

Keywords:
Antibiofilm
Jania rubens
Pathogenic bacteria
Sargassum dentifolium
Silver nanoparticles

ABSTRACT

Jania rubens and *Sargassum dentifolium* aqueous extracts were used as a reducing agent for the synthesis of silver nanoparticles (Ag-NPs). The prepared Ag-NPs have two plasmon absorption bands at 440 nm and 420 nm, with a direct band gap 2.25 eV and 2.38 eV for Ag-NPs/*J. rubens* and Ag-NPs/*S. dentifolium* respectively. From the FTIR results, the reduction has mostly been carried out by C=N, hydroxyl or sulfated polysaccharides groups present in *J. rubens* and *S. dentifolium*, respectively. TEM images shown that most particles are spherical in shape with no aggregations or debris were detected. The concentration of *S. dentifolium*/NPs showed approximately 2-fold than *J. Rubens*/NPs (470 and 240 $\times$ 10^3 NPs/ml) and an average particle size of 113 and 155 nm, respectively. A high repulsive and attractive forces between each nanoparticle were confirmed with an average zeta potential −24.7 and −28.2 mV for *J. rubens*/NPs and *S. dentifolium*/NPs, respectively. On the other hand, Ag-NPs concentrations of 10^4–10^5/ml were sufficient for killing *Salmonella typhimurium*, *Enterobacter aerogenes*, *Pseudomonas aeruginosa*, *Escherichia coli*, and the Gram-positive methicillin-resistant *Staphylococcus aureus*. Generally, both NPs showed reproducible, effective antibacterial activity with no significant differences between values of MIC and/or MBC for the two NPs against the tested pathogens. The results on biofilm formation implicate significant inhibition at the beginning of the adherence stage at various concentrations of Ag-NPs tested. Consequently, silver nanoparticles could be an effective antimicrobial agent without cause microbial resistance even after long-term usage.

1. Introduction

Nano-biotechnology is an evolving field that has made its contribution to all domains of human life [1–5]. Several physico-chemical approaches have been illustrated for the synthesis of metal nanoparticles [6–12]. A variety of green methods for synthesis of nanoparticles were needed because most of these means are inexpensive, non-toxic, eco-friendly and have easy production technology. The synthesis of new approaches for green nanoparticles from natural sources like plants [13,14] and algae [15–17]. For their easy availability, natural occurring, non-toxicity, the macroalgae have several potentials in the biosynthesis of silver nanoparticles such as eco-friendly, easy production technology and low costs [18]. El-Rafie et al. [1] demonstrated a fast, unexpensive, green easily amenable approach for biosynthesis of silver nanoparticles by reducing silver nitrate solution using marine macroalgae extract. Several macroalgae have been used for biosynthesis of Ag-NPs, particularly different *Sargassum spp.* [19,20] and *Jania rubens* [1]. It appears to be exceptionally sensible to trust silver nanoparticles biosynthesis as environmentally and ecologically safe as well as to enhance their antibacterial properties [14]. For metal nanoparticles, silver nanoparticles (Ag-NPs) have great efficacy as ideal antimicrobial agents [21]. Because of their antiseptic properties, the silver nanoparticles are widely used in the health-care sector and industrial applications [22–25]. On the other hand, Microbial activity in the environment is the main source of drinking water and foods spoilage, it is often responsible for severe diseases including the food-born one. Among these pathogenic bacteria, the *Enterobacter aerogenes, Escherichia coli, Pseudomonas aeruginosa, Salmonella typhimurium* and *Staphylococcus aureus* are biofilm forming organisms with a high multi-drug resistance against traditional antibiotics [26–30]. Antimicrobial agent against bacterial biofilm has been subjected to a considerable amount of work using green silver nanoparticles [13]. Although, a lot of work has been done on detecting the determinants of biofilm formation

* Corresponding author.
E-mail address: wesam.salem@svu.edu.eg (W. Salem).

https://doi.org/10.1016/j.ejbas.2017.10.006
2314-808X/

in vitro and, to some degree, the consequences of biofilms for persistence and pathogenicity *in vivo* [31].The biosynthesized nano-sized silver particles have a strong antibacterial activity for both Gram negative and positive bacteria. This makes silver metal an ideal alternative for different aims in the medical and biotechnological fields and may lead to important results for facing pathogenic microorganism and reduce the prevalence of illnesses caused by these bacterial strains [13]. The killing mechanism of Ag-NPs is due to the formation of free radicals that facilitate the induction of membrane damaging molecules [32]. Antimicrobial activity of Ag-NPs largely has been studied with human pathogenic bacteria, mainly *Escherichia coli* and *Staphylococcus aureus* [33], Enterotoxigenic *Escherichia coli* (ETEC) and *Vibrio cholerae* [13]. Hence, the present study was carried out to understand the anti-biofilm activity against some human pathogenic bacteria by (full-characterized) biosynthesized silver nanoparticles (Ag-NPs) using the aqueous extracts of two macro-algae, *Jania rubens* and *Sargassum dentifolium* which are the most common types of red and brown marine algae, respectively, present at the Red sea coast of Egypt.

2. Materials and methods

2.1. Macroalgae selection, collection and extract preparation

Jania rubens and *Sargassum dentifolium* macro-algae were collected by hand picking from the red sea in Hurghada, Egypt during May 2015. Healthy algal samples were cleaned from epiphytes, extraneous matter and necrotic were removed. Samples were washed thoroughly with sea water then sterile distilled water, air dried, cut into small pieces and then ground in a tissue grinder (IKA A 10, Germany) until reaching fine powder shape. Dried seaweed powder (1 g) was mixed with 100 ml of distilled water and heated to 100 °C, then filtered through Rotilabo® Tyb 601P filter paper.

2.2. Green synthesis of silver nanoparticles (Ag-NPs)

Ag-NPs were essentially synthesized as previously described [19]. A volume of 50 ml of 1 mM $AgNO_3$ solution was reacted with 50 ml of the aqueous extract of both algal extracts under continuous stirring at 45 °C. The solution changed color (brownish yellow to light purple) within 1 h, indicating the formation of Ag-NPs. For complete reaction, the obtained solution was left under stirring for a further 4 h. The Ag-NPs/*J. rubens* and/or *S. dentifolium* formed were separated from the residual seaweed by collecting the pellets after centrifugation at 6000 rpm/min for 10 min. The pellets were again suspended in double-distilled water and adjusted by adding 0.1 ml of phosphate buffer to the whole volume of physiological pH.

2.3. Characterization of nanoscale silver nanoparticles

The phyto-reduction of silver ions was monitored by recording the UV–Vis spectrum with a computerized double beam UV-2300 spectrophotometer with 5 nm steps. Measurements were performed at room temperature, in quartz cells, using silver nitrate (1 mM) as a blank, at normal incidence in the wavelength range 200–1100 nm. The reproducibility of the data was checked by measuring several specimens. The size and shape of silver nanoparticles were observed at 70 kV using "JEOL-2010, Japan" transmission electron microscope (TEM) equipped with digital "Kodak Megaplus® 1.6i camera" with image analysis and processing software (AMT, USA). Samples were prepared by placing a drop of each solution on carbon-coated copper grid and drying at room temperature as previously described by Salem et al. [14]. The infrared spectra of the macroalgae powder and of the green synthesized Ag-NPs were recorded on a Magna-FTIR 560 (USA) instrument at a resolution of 2 cm^{-1} range from 4000 to 400 cm^{-1} in KBr pellet using diffuse reflectance mode operated by Nicolet Omnic software as instructed by the manufacturers. The hydrodynamic diameters and Zeta potential of the biosynthesized Ag-NPs were measured using a Zetasizer Nano series compact scattering spectrometer (Malvern Instruments Ltd.; Malvern 6.32, UK).

2.4. Bacterial strains, culture conditions, and supplements

Human-pathogenic bacteria including the Gram-negative *Salmonella typhimurium* (ATCC14028), *Enterobacter aerogenes* (ATCC13048), *Pseudomonas aeruginosa* (ATCC278223), *Escherichia coli* (ATCC 25922) and the Gram-positive methicillin-resistant *Staphylococcus aureus* (MRSA, ATCC43300). Bacterial strains were maintained on Tryptic Soy Agar (TSA) slants and incubated at 37 °C for 24–48 h [34]. Three replicates of each microorganism were set up. The inocula were spread over TSA plates (10^7 CFU).

2.5. Determination of the minimum inhibitory concentration (MIC) and minimum bactericidal concentration (MBC)

Overnight (ON) cultures of the respective strains were grown in Tryptic Soy Broth (TSB) to an optical density at 595 nm (OD_{595}) of 1. Subcultures 1:1000 in (TSB). Samples of 100 μl bacterial cultures were placed into 96-well plates (F bottom, Sterilin) and 10 μl of appropriate serial dilutions of Ag-NPs (NPs/ml) was added. After 24 h incubation in a humid chamber at 37 °C, the optical density (OD_{595}) was measured using the "SPECTRONIC® GENESYS™ 2PC" Spectrophotometer, Spectronic Instruments, USA. To confirm bacterial growth inhibition and determine lack of metabolic activity, 40 μL of *p*-iodonitrotetrazolium violet (INT, 0.2 mg/ml, Sigma–Aldrich) was added to microplate wells and re-incubated for 30 min at 37 °C [35]. The MIC in the INT assay was defined as the lowest concentration of NPs that prevented color change as described earlier [36]. Growth was defined by an at least 2-fold increase of the OD_{595} compared to the negative control (TSA only). Next, MBC testing was performed, the bactericidal effect was defined as a 99.9% decrease in CFU (3 logs) in the starting inoculum during a 24 h incubation. The MBC was determined by transferring 50 μl from each well of an overnight MIC plates to sterile (TSA) fresh plates. Viable colonies were counted after 24 h at 37 °C. The limit of detection for this assay was 10^1 CFU/mL.

2.6. Static biofilm assay

Static biofilms were performed in microtiter plates by crystal violet staining essentially as previously published by Seper et al. [37], with some modifications. Briefly, the respective strains were grown overnight on (TSA) plates, suspended in (TSB), adjusted to an OD_{595} of 0.02. 130 μl of this dilution were placed in a 96 well microtiter plate (U bottom, Sterilin) for 24 h at 37 °C. After 24 h, 10 μl of Ag-NPs colloidal solutions with concentrations of $\sim 10^5$ NPs/ml was added. The addition of 10 μl of the both macroalgae aqueous extracts served as control. Biofilm was stained with 0.1% crystal violet, solubilized in 96% ethanol and the OD_{595} was measured using Infinite® F50 Robotic (Ostrich) Microplate Reader to quantify the amount of biofilm.

2.7. Statistical analysis

Data were analyzed using the Mann-Whitney U test or a Kruskal-Wallis test followed by *post hoc* Dunn's multiple comparisons. Differences were considered significant at *P* values of $\leq .05$. For all statistical analyses, GraphPad Prism version 5 was used.

3. Results and discussion

3.1. Characterization of the nanoparticles

3.1.1. UV–Vis spectrophotometer analysis

Silver nanoparticles (Ag-NPs) were synthesized according to established protocols [19] using dried seaweed powder from *Jania rubens* and *Sargassum dentifolium* macroalgae. Resulting in the two different sources of nanoparticles Ag-NPs/*J. rubens* and/or *S. dentifolium*. Throughout the study, NPs have been prepared several times without dramatic changes in yield or quality, suggesting a reproducible production of the NPs. The reaction was completed within 60 min which indicated by color changes of the silver nitrate solution after addition of aqueous extracts of both algae. In contrast, no change of color for the silver nitrate solution (control) without extracts. The intensity of colors steadily increased along the incubation period. Finally, Ag-NPs/*J. rubens* and/or *S. dentifolium* solutions exhibited a brownish yellow to light purple color respectively. The reduction of silver nitrate and excitation of surface plasmon resonance could be responsible for color reaction change [38]. UV–Vis spectrometer is spectral techniques are widely used to confirm the formation and structural characterization of nanoparticles in colloidal solution [39,40]. The UV–Vis spectroscopy was used for the confirmation of silver ions reduction by aqueous extracts to form Ag-NPs (Fig. 1A). A wavelength scan in the UV–Vis spectra revealed an absorption peak at approximately $\lambda = 440$ for Ag-NPs/*J. rubens* (Fig. 1A). Furthermore, Ag-NPs/*S. dentifolium* exhibited characteristics absorption peaks at approximately $\lambda = 420$ nm as previously published [19,41]. Optical absorption spectra of Ag-NPs are clearly dominated by surface plasmon within a shift to the red and/or blue end depends on particle size, morphology, the state of aggregation and the coating dielectric medium [42]. Interestingly, the prepared Ag-NPs have two plasmon absorption band, one at 295 nm for the both extracts, and the second at 440 nm and 420 nm for Ag-NPs prepared from *J. Rubens* and *S. dentifolium* extracts respectively. The plasmon absorption bands are the characteristics bands for Ag nanoparticles [42,43], which confirm that we obtain Ag nanoparticles. A surface plasmon absorption band appeared at 420 nm and 440 nm for Ag-NPs extracts indicating the presence of spherical or roughly spherical Silver nanoparticles [44]. As described in Fig. 1B, the transmittance for Ag-NPs decreases with the increase of the wavelength till 440 nm after this wavelength the transmittance increases, these results indicates transparent Ag-NPs. The value and nature of the optical band gap could be detected from the absorption, which corresponds to electron excitation from the valence to conduction bands. The relation between the absorption coefficients (α) and the incident photon energy ($h\nu$) can be written as $(\alpha h\nu)^{1/n} = A(h\nu - E_g)$ [45] where A is a constant and E_g is the band gap of the material and exponent n depends on the type of transition. For direct allowed n = 1/2, indirect allowed transition, n = 2, and for direct forbidden, n = 3/2. Fig. 1C depicts the relations between $(\alpha h\nu)^2$ and photon energy to determine the direct allowed band gap. These results clearly indicate that the direct band gap is 2.25 eV and 2.38 eV for Ag-NPs/*J. rubens* and Ag-NPs/*S. dentifolium* respectively.

3.1.2. FTIR studies

The FTIR spectra were used to identify the possible functional biomolecules responsible for the reduction of the Ag^+ ions and capping of the macroalgae formed Ag-NPs. Fig. 2 shows the FTIR spectra of *J. rubens* (Fig. 2A) and/or *S. dentifolium* (Fig. 2B) aqueous extracts and its bio-synthesized Ag-NPs. In the FTIR spectrum of *J. Rubens* extract, the signal at 1635 cm^{-1} corresponded to asymmetric stretching vibration of a C=N and band at 2834 and/or 2920 cm^{-1} attributed to symmetric CH- aliphatic vibration associated with aliphatic groups [46] or the C—OH, which disappeared after synthesis of Ag-NPs. This specified the involvement of C=N or hydroxyl groups in the reduction process of Ag-NPs. In addition, the peaks at 3420 cm^{-1} (OH stretching) was also detected. After reduction of $AgNO_3$, the decreases in intensity at 3397 cm^{-1} imply the involvement of the OH group in the reduction process. This is further confirmed with a reduction in PH of solution during the reaction. The sulfated polysaccharides peaks pointed out the involvement of sulfate groups in the biosynthesis of silver nanoparticles [19]. In agreement with that, Mahdavi et al. [47] and Venkatpurwar and Pokharkar's [48] stated that the sulfated polysaccharides in marine algae *S. muticum* and *Porphyra vietnamensis* had strong ability to synthesis of NPs. For FTIR spectra of *S. dentifolium* (Fig. 2B), the peaks at 1426 cm^{-1} indicate the C=C

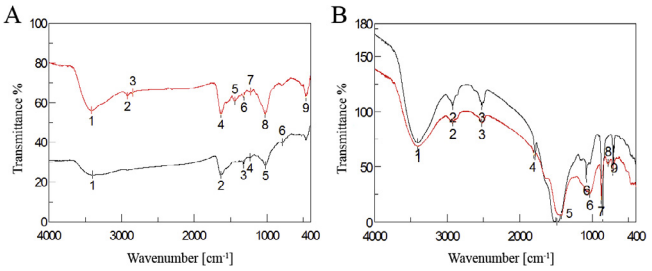

Fig. 2. Fourier Transform Infrared Spectroscopy (FTIR) Spectrum of biosynthesized silver nanoparticles. (A) Ag-NPs/*Jania rubens* (black line) and its algal extract (red line) (B) Ag-NPs/*Sargassum dentifolium* (black line) and its algal extract (red line) showing bioactive functional groups.

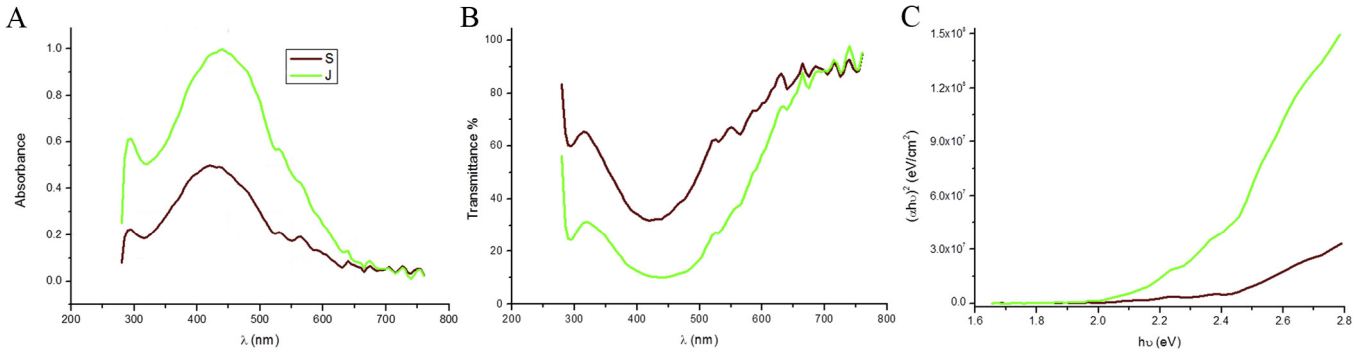

Fig. 1. Spectra analysis for biosynthesized silver nanoparticles (Ag-NPs). Shown are the UV–Vis absorption spectra from 200 to 800 nm of (A) Ag-NPs/*Jania rubens* (green line) and Ag-NPs/*Sargassum dentifolium* (brown line); (B) the dependence of transmittance on the wave length. (C) The relations between $(\alpha h\nu)^2$ and photon energy to determine the directly allowed band gap for both synthesized Ag-NPs.

groups derived from aromatic rings that are present in the *S. dentifolium* aqueous extract. Another peak at 1634 cm^{-1} is attributed to the stretching vibration of (NH) C=O group that is characteristic of proteins was shifted and became shorter after synthesis of Ag-NPs, approved that a member of (NH) C=O group is contributed in capping the nanoparticles synthesis. Hence, the FTIR results elucidated that the Ag-NPs were successfully synthesized and coated with bio-compounds present in both algal extracts by using a green approachs.

3.1.3. TEM and particles size distribution analysis

TEM measurements of the synthesized nanoparticles give a clear idea of the shape and size of the Ag-NPs produced extracellularly by *J. Rubens* and *S. dentifolium* extracts. As seen in Fig. 3 most the particles are spherical in shape. Few ellipsoidal and irregular silver nanoparticles can also be noticed. The exact size distribution and concentration of NPs in the preparations used in the assays throughout the study was determined by Zetasizer Nano series compact scattering spectrometer (Fig. 3). In general, *S. dentifolium*/NPs preparations showed approximately 2-fold concentrations than *J. Rubens*/NPs. (470 and 240×10^3 NPs/ml respectively), and average particle size of 113–155 nm. No aggregations or debris were detected by visualization of the nanoparticles within the TEM images (Fig. 3), which indicates the purity and uniformity of the colloidal solution of nanoparticles. Control of the size and structure of the resultant nanoparticles could be related to the interactions between bio-compounds such as polysaccharides, proteins, polyphenols and phenolic compounds and metal atoms [49].

3.1.4. Zeta potential (ZP)

Fig. 3 shows the ZP of the bio-synthesized Ag-NPs. The average ZP was −24.7 and −28.2 mV for Ag-NPs/*J. rubens* (Fig. 3A) and Ag-NPs/*S. dentifolium* (Fig. 3B) respectively. From the average ZP values, it is suggested that the bio-synthesized Ag-NPs were stable and wrapped with anionic compounds and responsible for electrostatic stabilization. This might be achieved by the help of high repulsive and attractive forces between nanoparticles [50]. Negative charge on surface of nanoparticles results in repulsion among the nanoparticles leading to stability of nanoparticles in cell culture media [51].

3.2. Efficacy of Ag-NPs against some human pathogenic bacteria

The antibacterial activities of the two synthesized Ag-NPs mediated by *J. rubens* and *S. dentifolium* extracts were studied against the most dominant bacterial causative agents for a human. Minimal inhibitory concentration (MIC) and/or minimal bactericidal concentration (MBC) assays were statistically analyzed for that target (Fig. 4). For MIC, a colorimetric INT-formazan assay, which allows detection of viable bacteria by their respiratory activity was assessed [52,53]. Interestingly, no significant differences between values of MIC and/or MBC for the two NPs against the tested pathogens (Fig. 4). In detail, Ag-NPs concentrations of 10^4–10^5/ml were sufficient for the killing of all the tested Gram-negative and positive bacteria (Fig. 4A and B). Silver nanoparticles can cause growth inhibition or cell lysis via various mechanisms [32,54]. The lethal effect of silver for bacteria can also be elucidated by thiol group reactions that inactivate enzymes [55,56]. Also, Steuber et al. [57] proposed a mechanism for Ag^+ action in *Vibrio alginolyticus* involving the direct displacement of FAD from the holoenzyme Na^+-NQR, which results in loss of enzyme activity. In addition, silver treatments inhibits DNA replication, ribosomal molecules and expression of extracellular proteins, moreover, it could be interferes with the respiratory chain of microorganisms [56,58,59].

3.2.1. Macroalgae extracts and Ag-NPs have inverse effects on biofilm formation

Biofilm formation by pathogenic bacteria has been the area of a severity amount of experimental work. Since biofilms are generally known to promote resistance to several antimicrobial agents, we

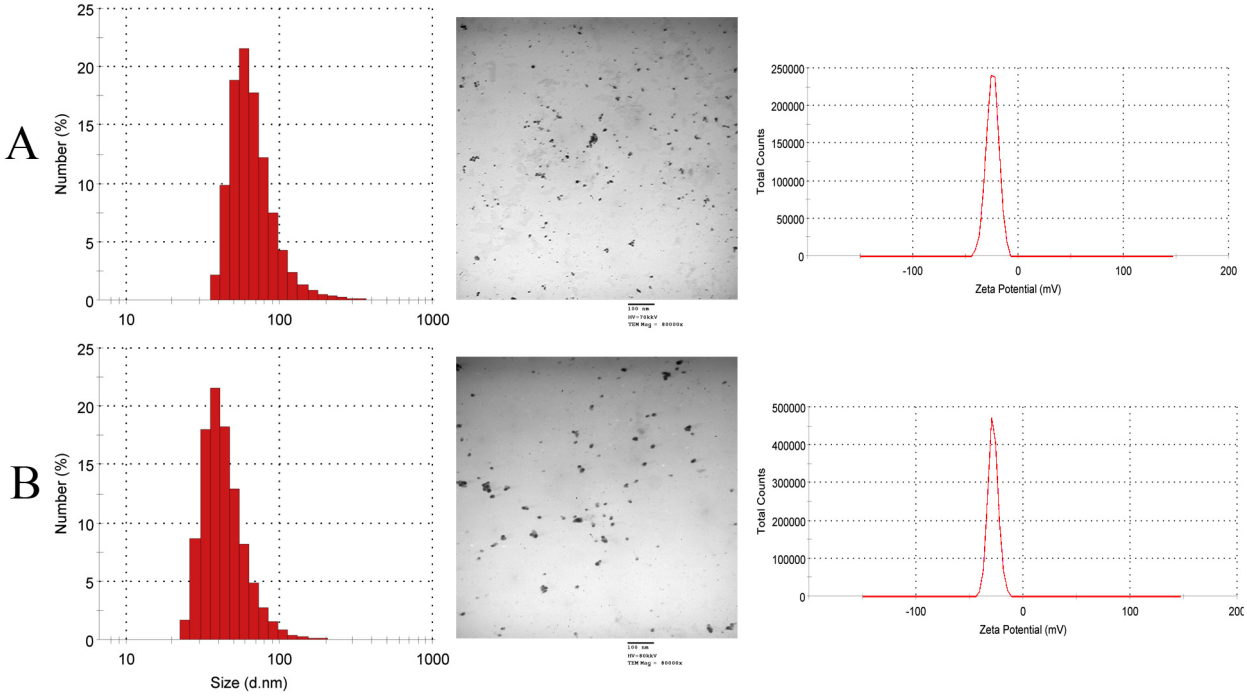

Fig. 3. TEM images with the corresponding size distribution and zeta potential for biosynthesized silver nanoparticles. (A) Ag-NPs/*Jania rubens* and (B) Ag-NPs/*Sargassum dentifolium*.

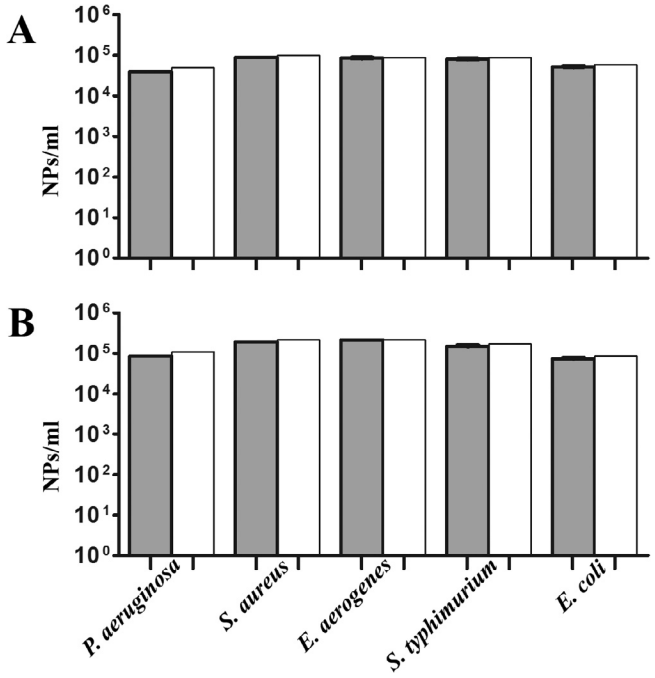

Fig. 4. Efficacy of Ag-NPs expressed as MIC and MBC assay reduction. MIC_{90} determination of Ag-NPs against some pathogenic bacteria (A) Ag-NPs/*Jania rubens* (B) Ag-NPs/*Sargassum dentifolium* were determined by measuring OD_{600} nm for MIC by tetrazolium reduction assay (gray) and were confirmed as MBC by colony count (white). Shown are the medians from at least eight independent measurements. The error bars indicate the interquartile range.

analyzed the impact of Ag-NPs on human-pathogenic bacteria such as *S. typhimurium*, *E. aerogenes*, *P. aeruginosa*, *E. coli* and the Gram-positive methicillin-resistant *S. aureus*. Therefore, we allowed the five tested pathogens to from static biofilms for 24 h before Ag-NPs were added. The addition of *J. Rubens* and *S. dentifolium* extracts served as a positive control, respectively. Finally, after an additional incubation period of 24 h the biofilm amount was quantified by crystal violet staining (Fig. 5). Among the five tested bacterial strains, the addition of Ag-NPs significantly reduced the biofilm amount compared to control, the exception is *S. aureus* in the case of Ag-NPs/*S. dentifolium*. Interestingly, the two Ag-NPs showed a highly significant difference compared to the original macroalgal extracts, except for *P. aeruginosa* (Fig. 5). Notably, the two macroalgal extracts showed no change in the biofilm formation for all five tested pathogens compared to control (original biofilm), the exception is *E. coli* with both extracts, and *S. typhimurium* with *J. Rubens* extract. Although both NPs exhibited robust antibacterial activity in the MIC by INT assays and MBC; the Ag-NPs/*J. rubens* generally showed a slightly higher efficacy against all pathogens compared to Ag-NPs/*S. dentifolium* that affected only Gram-negative bacteria. At 24 h of incubation, the Ag-NPs depicted the weak adherence and disintegrated biofilm of the test bacterial strains, in control, the strong adhering ability of bacterial biofilm led to the development of dense biofilm formation on the 96-microplate was observed. Thus Ag-NPs were active positively in clearing the establishment of the bacterial biofilm [60]. Also, the protein biosynthesis of stabilized Ag-NPs coated with polycaprolactam (polymer) proved to be a good anti-biofilm agent against pathogenic bacteria. [61]. The same technique was adopted earlier to measure the biofilm inhibition and adherences against *Streptococcus pyogenes* [62], *Staphylococcus aureus* [63,64], and *E. coli* [65] using different bacterial extracts. The coated nanoparticles on the surfaces, surfactants, and enzymes inhibited the bacterial biofilm formation [66] Same results were recorded earlier as against *Vibrio cholerae* and enterotoxigenic *Escherichia coli* using Ag-NPs synthesized from *Calotropis procera* [13]. Noteworthy, bacterial biofilms cause chronic infections because they show increased resistance against antibiotics, chemicals and phagocytosis [67]. Thus, the failer of antibiotic penetration within the bacterial biofilm matrix resulted to the bacterial biofilms resistence against these antibiotics [68]. The above-mentioned attributes of bacterial biofilms place them along with the most dangerous problems, which medicine is currently challenged. The results implicate that the biofilm formation was possibly inhibited at the beginning of the adherence stage at various concentrations of Ag-NPs tested. Consistent with our results, Ag-NPs have been recently shown to inhibit and reduce biofilm formations of several bacterial species [69].

4. Conclusion

Ag-NPs offer an inexpensive alternative approach to reducing the infectious dose of the most common food-born pathogens. The quick and ready synthesis of nanoparticles does not require specially trained staff or expensive tools and is likely to be

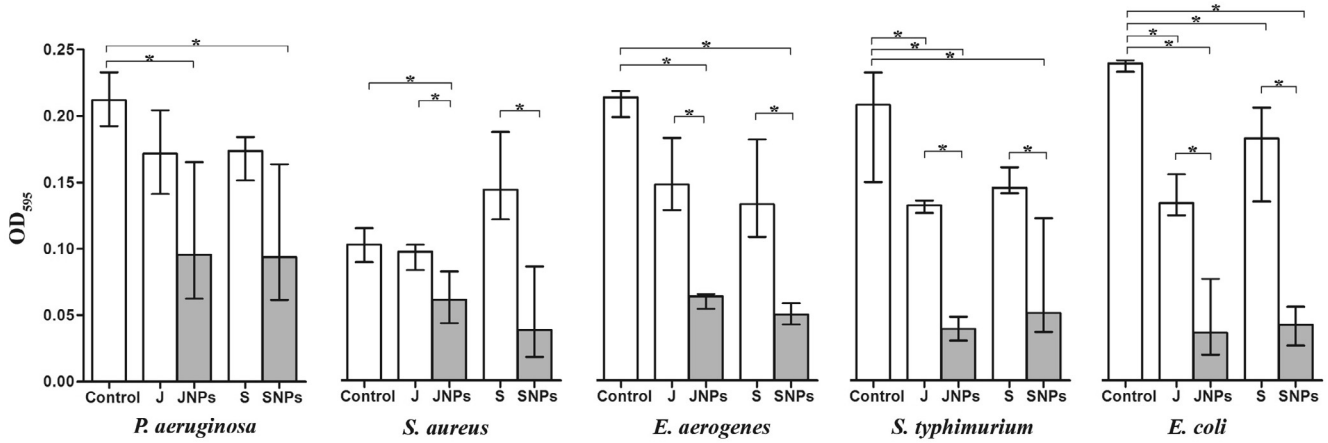

Fig. 5. Alterations of static biofilm formation treated with Ag-NPs. The biofilm formation capacity of some pathogenic bacteria was quantified after 24 h post inoculations with Ag-NPs/*Jania rubens* (JNPs) and Ag-NPs/*Sargassum dentifolium* (SNPs) compared to macro-algae extracts; *J. rubens* (J) or *S. dentifolium* (S) under static conditions by crystal violet staining and subsequent determination of the OD_{595}. Shown are the medians from at least eight independent measurements. The error bars indicate the interquartile range.

performed in epidemic areas. Interestingly, long time-exposure of bacteria to Ag-NPs act against developing of resistant bacteria so far.

References

[1] El-Rafie HM, El-Rafie MH, Zahran MK. Green synthesis of silver nanoparticles using polysaccharides extracted from marine macro algae. Carbohydr Polym 2013;96:403–10. doi: https://doi.org/10.1016/j.carbpol.2013.03.071.

[2] Goudarzi M, Bazarganipour M, Salavati-Niasari M. Synthesis, characterization and degradation of organic dye over Co_3O_4 nanoparticles prepared from new binuclear complex precursors. RSC Adv 2014;4:46517–20. doi: https://doi.org/10.1039/C4RA09653C.

[3] Goudarzi M, Mir N, Mousavi-Kamazani M, Bagheri S, Salavati-Niasari M. Biosynthesis and characterization of silver nanoparticles prepared from two novel natural precursors by facile thermal decomposition methods. Sci Rep 2016;6:32539.

[4] Goudarzi M, Ghanbari D, Salavati-Niasari M, Ahmadi A. Synthesis and characterization of Al(OH)3, Al_2O_3 nanoparticles and polymeric nanocomposites. J Cluster Sci 2016;27:25–38. doi: https://doi.org/10.1007/s10876-015-0895-5.

[5] Goudarzi M, Salavati-Niasari M, Motaghedifard M, Hosseinpour-Mashkani SM. Semiconductive Tl_2O_3 nanoparticles: facile synthesis in liquid phase, characterization and its applications as photocatalytic substrate and electrochemical sensor. J Mol Liq 2016;219:720–7. doi: https://doi.org/10.1016/j.molliq.2016.04.007.

[6] Sailaja A, Amareshwar P, Chakravarty P. Different techniques used for the preparation of nanoparticles using natural polymers and their application. Int J Pharm Pharm Sci 2011;3:45–50.

[7] Rodríguez-Sánchez L, Blanco MC, López-Quintela MA. Electrochemical synthesis of silver nanoparticles. J Phys Chem B 2000;104:9683–8. doi: https://doi.org/10.1021/jp001761r.

[8] Gao Y, Cranston R. Recent advances in antimicrobial treatments of textiles. Text Res J 2008;78:60–72. doi: https://doi.org/10.1177/0040517507082332.

[9] Goudarzi M, Ghanbari D, Salavati-niasari M. Room temperature preparation of aluminum hydroxide nanoparticles and flame retardant poly vinyl alcohol nanocomposite. J Nanostruct 2015;5:110–5. doi: https://doi.org/10.7508/jns.2015.02.005.

[10] Mousavi-Kamazani M, Salavati-Niasari M, Hosseinpour-Mashkani SM, Goudarzi M. Synthesis and characterization of $CuInS_2$ quantum dot in the presence of novel precursors and its application in dyes solar cells. Mater Lett 2015;145:99–103. doi: https://doi.org/10.1016/j.matlet.2015.01.076.

[11] Mousavi-Kamazani M, Salavati-Niasari M, Goudarzi M, Zarghami Z. Hydrothermal synthesis of CdIn nanostructures using new starting reagent for elevating solar cells efficiency. J Mol Liq 2017;242:653–61. doi: https://doi.org/10.1016/j.molliq.2017.07.059.

[12] Goudarzi M, Mousavi-Kamazani M, Salavati-Niasari M. Zinc oxide nanoparticles: solvent-free synthesis, characterization and application as heterogeneous nanocatalyst for photodegradation of dye from aqueous phase. J Mater Sci Mater Electron 2017;28:8423–8. doi: https://doi.org/10.1007/s10854-017-6560-z.

[13] Salem W, Leitner DR, Zingl FG, Schratter G, Prassl R, Goessler W, et al. International journal of medical microbiology antibacterial activity of silver and zinc nanoparticles against *Vibrio cholerae* and enterotoxic *Escherichia coli*. Int J Microbiol 2015;305:85–95.

[14] Salem WM, Haridy M, Sayed WF, Hassan NH. Antibacterial activity of silver nanoparticles synthesized from latex and leaf extract of *Ficus sycomorus*. Ind Crops Prod 2014;62:228–34. doi: https://doi.org/10.1016/j.indcrop.2014.08.030.

[15] Sahayaraj K, Rajesh S, Rathi JM. Silver nanoparticles biosynthesis using marine alga Padina pavonica (Linn.) and its microbicidal activity. Dig J Nanomater Biostruct 2012;7:1557–67.

[16] El-Sheekh MM, El-Kassas HY. Application of biosynthesized silver nanoparticles against a cancer promoter cyanobacterium, *Microcystis aeruginosa*. Asian Pac J Cancer Prev 2014;15:6773–9. doi: https://doi.org/10.7314/APJCP.2014.15.16.6773.

[17] Eh Y, Am A, Gs M. Green synthesis of iron oxide (Fe3O4) nanoparticles using two selected brown seaweeds: characterization and application for lead bioremediation. Acta Oceanol Sin 2016. doi: https://doi.org/10.1007/s13131-016-0880-3.

[18] Velgosová O, Mražíková A, Marcinčáková R. Influence of pH on green synthesis of Ag nanoparticles. Mater Lett 2016;180:336–9. doi: https://doi.org/10.1016/j.matlet.2016.04.045.

[19] Azizi S, Namvar F, Mahdavi M, Bin AM, Mohamad R. Biosynthesis of silver nanoparticles using brown marine macroalga, *Sargassum muticum* aqueous extract. Materials 2013;6:5942.

[20] Rajeshkumar S, Malarkodi C, Paulkumar K, Vanaja M, Gnanajobitha G, Annadurai G. Algae mediated green fabrication of silver nanoparticles and examination of its antifungal activity against clinical pathogens. Int J Metals 2014;2014:1–8. doi: https://doi.org/10.1155/2014/692643.

[21] Cho K-H, Park J-E, Osaka T, Park S-G. The study of antimicrobial activity and preservative effects of nanosilver ingredient. Electrochimica 2005;51:956–60.

[22] Reidy B, Haase A, Luch A, Dawson K, Lynch I. Mechanism of silver nanoparticle release, transformation and toxicity: a critical review of current knowledge and recommendations for future studies and applications. Materials 2013;6:2295. doi: https://doi.org/10.3390/ma6062295.

[23] Le Ouay B, Stellacci F. Antibacterial activity of silver nanoparticles: a surface science insight. Nano Today 2015;10:339–54. doi: https://doi.org/10.1016/j.nantod.2015.04.002.

[24] Haider A, Kang I. Preparation of silver nanoparticles and their industrial and biomedical applications: a comprehensive review. Adv Mater Sci Eng 2015;2015:16.

[25] Pugliara A, Makasheva K, Despax B, Bayle M, Carles R, Benzo P, et al. Assessing bio-available silver released from silver nanoparticles embedded in silica layers using the green algae *Chlamydomonas reinhardtii* as bio-sensors. Sci Total Environ 2015;565:863–71. doi: https://doi.org/10.1016/j.scitotenv.2016.02.141.

[26] Davin-Regli A, Bolla J-M, James CE, Lavigne J-P, Chevalier J, Garnotel E, et al. Membrane permeability and regulation of drug "influx and efflux" in enterobacterial pathogens. Curr Drug Targets 2008;9:750–9. doi: https://doi.org/10.2174/138945008785747824.

[27] Nabet C, Raoult D. The hidden epidemic of *Escherichia coli*. Clin Microbiol Infect 2014;20:O792–3. doi: https://doi.org/10.1111/1469-0691.12757.

[28] Lautenbach E, Weiner MG, Nachamkin I, Bilker WB, Sheridan A, Fishman NO. Imipenem resistance among *Pseudomonas aeruginosa* isolates: risk factors for infection and impact of resistance on clinical and economic outcomes. Infect Control Hosp Epidemiol 2006;27:893–900. doi: https://doi.org/10.1086/507274.

[29] Harish BN, Menezes GA. Determination of antimicrobial resistance in *Salmonella* spp.. Methods Mol Biol 2015;1225:47–61.

[30] Kuroda H, Kuroda M, Cui L, Hiramatsu K. Subinhibitory concentrations of β-lactam induce haemolytic activity in *Staphylococcus aureus* through the SaeRS two-component system. FEMS Microbiol Lett 2007;268:98–105. doi: https://doi.org/10.1111/j.1574-6968.2006.00568.x.

[31] Joo H-S, Otto M. Molecular basis of in-vivo biofilm formation by bacterial pathogens. Chem Biol 2013;19:1503–13. doi: https://doi.org/10.1016/j.chembiol.2012.10.022.Molecular.

[32] Kim JS, Kuk E, Yu KN, Kim J, Park SJ, Lee HJ, et al. Antimicrobial effects of silver nanoparticles. Nanomed Nanotechnol Biol Med 2007;3:95–101. doi: https://doi.org/10.1016/j.nano.2006.12.001.

[33] Shrivastava S, Bera T, Roy A, Singh G, Ramachandrarao P, Dash D. Characterization of enhanced antibacterial effects of novel silver nanoparticles. Nanotechnology 2010;18:1–9. doi: https://doi.org/10.1088/0957-4484/18/22/225103.

[34] Mueller JH, Hinton J. A protein-free medium for primary isolation of the *Gonococcus* and *Meningococcus*. Exp Biol Med 1941;48:330–3. doi: https://doi.org/10.3181/00379727-48-13311.

[35] Ellof J. A quick microplate method to determine the minimum inhibitory sensitive and concentration of plant extracts for bacteria. Planta Med 1998;64:711–3.

[36] Lall N, Henley-Smith CJ, De Canha MN, Oosthuizen CB, Berrington D. Viability reagent, prestoblue, in comparison with other available reagents, utilized in cytotoxicity and antimicrobial assays. Int J Microbiol 2013;2013. doi: https://doi.org/10.1155/2013/420601.

[37] Seper A, Fengler VHI, Roier S, Wolinski H, Kohlwein SD, Bishop AL, et al. Extracellular nucleases and extracellular DNA play important roles in *Vibrio cholerae* biofilm formation. Mol Microbiol 2011;82:1015–37. doi: https://doi.org/10.1111/j.1365-2958.2011.07867.x.

[38] Mulvaney P, Perera J, Biggs S, Grieser F, Stevens G. The direct measurement of the forces of interaction between a colloid particle and an oil droplet. J Colloid Interface Sci 1996;183:614–6. doi: https://doi.org/10.1006/jcis.1996.0588.

[39] El-raady AAABD, Abo-bakr AM. On the effect of complexing agents on the structural and optical properties of cds nanocrystals. Chalcogenide Lett 2013;10:55–62.

[40] Massaud Mostafa A. Laser effect on particle size of Barium Titanate nanoparticles \nprepared by a Sol-Gel Method. IOSR J Appl Phys (IOSR-JAP) 2014;6:46–9.

[41] Jeeva K, Thiyagarajan M, Elangovan V, Geetha N, Venkatachalam P. *Caesalpinia coriaria* leaf extracts mediated biosynthesis of metallic silver nanoparticles and their antibacterial activity against clinically isolated pathogens. Ind Crops Prod 2014;52:714–20. doi: https://doi.org/10.1016/j.indcrop.2013.11.037.

[42] Mahmudin L, Suharyadi E, Bambang A, Utomo S, Abraha K. Optical properties of silver nanoparticles for surface plasmon resonance (spr)-based biosensor applications. J Modern Phys 2015;6:1071–6. doi: https://doi.org/10.4236/jmp.2015.68111.

[43] Budhiraja N, Sharma A, Dahiya S, Parmar R. Synthesis and optical characteristics of silver nanoparticles on different substrates. Lett Chem Ellipsis 2013;14:80–8. doi: https://doi.org/10.18052/www.scipress.com/ILCPA.19.80.

[44] Guzmán MGM, Dille J, Godet S. Synthesis of silver nanoparticles by chemical reduction method and their antibacterial activity. Int Sholarly Sci Res Innovation 2008;2:91–8. doi: https://doi.org/10.1007/s11814-010-0067-0.

[45] Tauc J, Grigorovici R, Vancu A. Optical properties and electronic structure of amorphous Germanium. Phys Status Solidi (B) 1966;15:627–37. doi: https://doi.org/10.1002/pssb.19660150224.

[46] Camara RBG, Costa LS, Fidelis GP, Nobre LTDB, Dantas-Santos N, Cordeiro SL, et al. Heterofucans from the brown seaweed *Canistrocarpus cervicornis* with anticoagulant and antioxidant activities. Mar Drugs 2011;9:124–38. doi: https://doi.org/10.3390/md9010124.

[47] Mahdavi M, Namvar F, Bin AM, Mohamad R. Green biosynthesis and characterization of magnetic iron oxide ($Fe3O_4$) nanoparticles using seaweed (*Sargassum muticum*) aqueous extract. Molecules 2013;18:5954–64.
[48] Venkatpurwar V, Pokharkar V. Green synthesis of silver nanoparticles using marine polysaccharide: study of in-vitro antibacterial activity. Mater Lett 2011;65:999–1002. doi: https://doi.org/10.1016/j.matlet.2010.12.057.
[49] Shao Y, Jin Y, Dong S. Synthesis of gold nanoplates by aspartate reduction of gold chloride. Chem Commun 2004:1104–5.
[50] Lee JJ, Kim HY, Zhou H, Hwang S, Koh K, Han D-W, et al. Green synthesis of phytochemical-stabilized Au nanoparticles under ambient conditions and their biocompatibility and antioxidative activity. J Mater Chem 2011;21:13316–26. doi: https://doi.org/10.1039/c1jm11592h.
[51] Moore TL, Rodriguez-Lorenzo L, Hirsch V, Balog S, Urban D, Jud C, et al. Nanoparticle colloidal stability in cell culture media and impact on cellular interactions. Chem Soc Rev 2015;44:6287–305. doi: https://doi.org/10.1039/c4cs00487f.
[52] Mann CM, Markham JL. A new method for determining the minimum inhibitory concentration of essential oils. J Appl Microbiol 1998;84:538–44. doi: https://doi.org/10.1046/j.1365-2672.1998.00379.x.
[53] Palomino JC, Martin A, Camacho M, Guerra H, Swings J, Portaels F. Resazurin microtiter assay plate: simple and inexpensive method for detection of drug resistance in *Mycobacterium tuberculosis*. Antimicrob Agents Chemother 2002;46:2720–2.
[54] Prabhu S, Poulose EK. Silver nanoparticles: mechanism of antimicrobial action, synthesis, medical applications, and toxicity effects. Int Nano Lett 2012;2:32. doi: https://doi.org/10.1186/2228-5326-2-32.
[55] Chen X, Schluesener H. Nanosilver: a nanoproduct in medical application. Toxicol Lett 2008;176:1–12.
[56] Feng QL, Wu J, Chen GQ, Cui FZ, Kim TN, Kim JO. A mechanistic study of the antibacterial effect of silver ions on *Escherichia coli* and *Staphylococcus aureus*. J Biomed Mater Res 2001:662–8.
[57] Steuber J, Krebs W, Dimroth P. The Na+-translocating NADH:ubiquinone oxidoreductase from *Vibrio alginolyticus*-redox states of the FAD prosthetic group and mechanism of Ag^+ inhibition. Eur J Biochem/FEBS 1997;249:770–6. doi: https://doi.org/10.1111/j.1432-1033.1997.t01-2-00770.x.
[58] Rainnie DJ, Bragg P, Bragg PD, Rainnie DJ. The effect of silver ions on the respiratory chain of *Escherichia coli*. Can J Microbiol 1974;20:883–9. doi: https://doi.org/10.1139/m74-135.
[59] Yamanaka M, Hara K, Kudo J. Bactericidal actions of a silver ion solution on escherichia coli, studied by energy-filtering transmission electron microscopy and proteomic analysis bactericidal actions of a silver ion solution on *Escherichia coli,* studied by energy-filtering transmi. Appl Environ Microbiol 2005;71:7589–93. doi: https://doi.org/10.1128/AEM.71.11.7589.
[60] Martinez-Gutierrez F, Boegli L, Agostinho A, Sánchez EM, Bach H, Ruiz F, et al. Anti-biofilm activity of silver nanoparticles against different microorganisms. https://doi.org/101080/089270142013794225; 2013.
[61] Prabhawathi V, Sivakumar PM, Doble M. Green synthesis of protein stabilized silver nanoparticles using *Pseudomonas fluorescens*, a marine bacterium, and its biomedical applications when coated on polycaprolactam. Ind Eng Chem Res 2012;51:5230–9. doi: https://doi.org/10.1021/ie2029392.
[62] Thenmozhi R, Nithyanand P, Rathna J, Pandian SK. Antibiofilm activity of coral associated bacteria against different clinical M serotypes of *Streptococcus pyogenes*. FEMS Immunol Med Microbiol 2009;57:284–94.
[63] Gowrishankar S, Duncun Mosioma N, Karutha Pandian S. Coral-associated bacteria as a promising antibiofilm agent against methicillin-resistant and -susceptible Staphylococcus aureus biofilms. Evid Based Complement Altern Med 2012;2012. doi: https://doi.org/10.1155/2012/862374.
[64] Bakkiyaraj D, Pandian SK. In vitro and in vivo antibiofilm activity of a coral associated actinomycete against drug resistant *Staphylococcus aureus* biofilms. Biofouling 2010;26:711–7. doi: https://doi.org/10.1080/08927014.2010.511200.
[65] Sayem S, Manzo E, Ciavatta L, Tramice A, Cordone A, Zanfardino A, et al. Anti-biofilm activity of an exopolysaccharide from a sponge-associated strain of *Bacillus licheniformis*. Microb Cell Fact 2011;10:74. doi: https://doi.org/10.1186/1475-2859-10-74.
[66] Kaplan JB, Ragunath C, Velliyagounder K, Fine DH, Ramasubbu N. Enzymatic detachment of *Staphylococcus epidermidis* biofilms. Antimicrob Agents Chemother 2004;48:2633–6. doi: https://doi.org/10.1128/AAC.48.7.2633-2636.2004.
[67] Høiby N, Bjarnsholt T, Givskov M, Molin S, Ciofu O. Antibiotic resistance of bacterial biofilms. Int J Antimicrob Agents 2010;35:322–32. doi: https://doi.org/10.1016/j.ijantimicag.2009.12.011.
[68] Thien-fah CM, Toole GAO. Mechanisms of biofilm resistance to antimicrobial agents. Trends Microbiol 2001;9:34–9.
[69] Markowska K, Grudniak AM, Wolska KI. Silver nanoparticles as an alternative strategy against bacterial biofilms. Acta Biochim Pol 2013;60:523–30.